



**Here is a sample chapter
from this book.**

**This sample chapter is copyrighted
and made available for personal use
only. No part of this chapter may be
reproduced or distributed in any
form or by any means without the
prior written permission of Medical
Physics Publishing.**

6

Treatment Planning Considerations Using IMRT

Margie A. Hunt
Chandra M. Burman

Introduction	103
IMRT or 3DCRT?	105
The MSKCC IMRT Planning Process.....	107
Patient Selection • Patient Simulation And Structure Localization • Selection Of Beam Energy, Number, And Direction • Optimization • Conversion Of Intensity Profiles To Leaf Motion • Forward Dose Calculation And Plan Evaluation • IMRT Plan Documentation And QA	
Controlling Dose Distributions Designed Using Inverse Planning: Optimization Algorithm Performance	115
Optimization Parameters • Beam Selection • “Optimization Only” Structures	
Summary	118
References	119

Introduction

In radiation therapy, a tumoricidal dose must be delivered while minimizing the dose to the surrounding normal tissues. Although three-dimensional conformal radiation therapy (3DCRT), with its careful delineation of target and normal tissues and volumetric evaluation of dose, has facilitated an increased target dose and/or reduced normal tissue dose in certain sites (Armstrong et al. 1993), intensity modulated radiation therapy (IMRT) could lead to even greater improvements in the therapeutic ratio.

The concept of intensity-modulated fields created through inverse planning was first proposed by Brahme in 1988 (Brahme 1988). Given a set of beams and a desired dose distribution, the optimum shape of the beams could be determined by back projection, leading to non-uniform beam intensities. Although this particular optimization technique was limited by non-physical solutions characterized by negative ray weights, the utility of the technique, particularly for concave targets surrounding an organ at risk, was obvious. It was soon realized that intensity modulation was capable of producing highly complex, tightly conforming dose distributions. Since then, many computational techniques for determining the beam intensity profiles have been proposed, including gradient techniques (Bortfeld et al. 1990), maximal entropy and maximal likelihood optimization (Llacer 1997), simulated annealing (Rosen et al. 1995), and methods relying

on the genetic algorithm (Ezzell 1996). Some of these methods have been implemented in commercial planning systems including simulated annealing in CORVUS (NOMOS Corporation, Sewickley, PA) (Carol, Nash, and Campbell 1997) and gradient techniques in HELIOS (Varian Associates, Palo Alto, CA). The Memorial Sloan Kettering Cancer Center (MSKCC) optimization algorithm, developed by Spirou and Chui (1998) and discussed in detail in chapter 3, relies on a conjugate gradient minimization method and least-squares objective function.

Just as there are many optimization methods used to design IMRT plans, several methods exist for the delivery of intensity-modulated fields. Although physical compensators can be used (Purdy 1997), their fabrication is time consuming and their use is cumbersome. The relatively recent commercial availability of computer-controlled slit and multileaf collimators (MLCs) has made the delivery of intensity-modulated fields more practical. To date, extensive clinical experience exists for the following IMRT delivery methods: computer-controlled collimating slit device (Carol 1994), multiple static fields (i.e., the “step-and-shoot” method) (Galvin, Chen, and Smith 1993; Boyer et al. 1994), and dynamic multileaf collimation (DMLC) (Spirou and Chui 1994). Each method has its advantages and limitations, and although there exist some studies comparing delivery methods (Chui et al. 2001), there are really no available data that permit a true “head to head” comparison between the various IMRT techniques currently available.

Although the overall processes of IMRT and 3DCRT are quite similar, the philosophical basis of plan design differs significantly. One might say they are diametrically opposite in approach. Conventional 3DCRT treatment planning is forward based and manually optimized. That is, the treatment planner chooses all beam parameters, such as the number of beams, beam directions, shapes, weights, etc., and the computer merely calculates the resulting dose distribution. Based on the resulting dose distribution the planner intuitively iterates the various parameters in an attempt to optimize the dose distribution. A key point being, however, that the optimum, or desired dose distribution is never explicitly defined. Thus, an optimal 3DCRT plan, designed conventionally, is the result of an iterative manipulation of beam energy, weighting, and direction, and beam modifying devices such as blocks and wedges. Although computer-driven optimization of parameters such as beam direction (Vijayakumar et al. 1991; Soderstrom and Brahme 1992) and weighting (Langer and Leong 1987; Mageras and Mohan 1993) has been attempted, it has met only limited clinical success.

Conversely, with IMRT dose distributions are inversely determined, meaning that the treatment planner must specify in advance the dose distribution that is desired, and the computer then calculates a set of beam intensities that will produce, as nearly as possible, the desired dose distribution. Specification by the planner of the desired dose distribution is made by means of dose-volume constraints in which the planner defines for the computer minimum and maximum desirable doses for all structures in the plan [such as the CTV (clinical target volume), PTV (planning target volume), and radiosensitive normal tissues] plus a set of penalty weights to indicate the relative importance for meeting the specified dose constraints for each structure. For example, the planner could specify that meeting the dose constraints for the PTV are more important than for the spinal cord, or vice versa. Different penalty weights can also be applied to overdosing as opposed to underdosing certain structures. So, for IMRT the optimization parameters and structures are the primary variables used to control the dose distribution as opposed to the beam weights or shapes as in 3DCRT treatment planning. Specification of the optimization parameters and beam placement requires knowledge of how the details of the dose calculation algorithms and anatomical features of the patient such as the proximity of the normal tissues to the target affect the outcome of optimization. Hence, the combination of beams, optimization parameters, and structures needed to achieve the best plan are planning system and patient specific. Planners must develop an intuition as to how these factors affect optimized dose distributions.

This chapter will describe the general approach to treatment planning optimization that has been developed at MSKCC during the past 8 years. The techniques discussed have been found useful for the optimization algorithm and delivery methods used at our institution. Some of these techniques may not be relevant or be ineffective with other systems. A variety of site-specific information is discussed in this chapter to demonstrate general issues related to IMRT planning. Additional site-specific planning information will be found in the appropriate clinical chapters.

IMRT Or 3DCRT?

At the most basic level, IMRT could be considered in virtually all situations where there is a desire to either increase tumor dose or decrease normal tissue dose—that is, almost every site currently treated with external beam radiation therapy! However, there are increased costs associated with planning and delivering IMRT that must be considered. In addition to the necessary equipment costs, operating costs are higher (at least currently) and are proportional to the number of patients receiving IMRT treatment. Therefore, it makes sense to select sites for IMRT treatment that will reap the greatest benefit.

Multiple studies have now clearly demonstrated the value of IMRT in improving target coverage and decreasing normal tissue doses in clinical situations where concave targets surround normal tissues (Happersett et al. 1999, 2000; Burman et al. 1997; Fournier-Bidoz et al. 2001; Hunt et al. 2001; Wu et al. 2000; Chao et al. 2000; De Neve et al. 1999; Verhey 1999; Hsiung et al. 2002). Concave distributions created with IMRT have been used in prostate cancer (Zelevsky et al. 2000) to facilitate dose escalation with no increase in rectal dose and in head and neck cancer to decrease normal tissue morbidity, particularly to the parotid glands (Wu et al. 2000). As another example, consider the IMRT technique developed by Happersett et al. (2000) for the treatment of thyroid cancer. Historically, an extremely difficult site in which to achieve good dose distributions, successful treatment of thyroid carcinomas requires doses of 60 Gy or more to large target volumes including the thyroid bed and regional lymph nodes that surround the spinal cord. Happersett et al. developed an IMRT technique consisting of either five or six fields (figure 6–1) and compared it to anterior posterior/posterior anterior (AP/PA) opposed fields and a 3-D conformal plan for five patients. With IMRT the volume of the PTV receiving the prescription dose increased by 10% relative to the 3-D plan and 60% relative to AP/PA fields. Dose to the spinal cord was acceptable with all three techniques, but the volume of lung receiving in excess of 25 Gy was 10% to 15% less with IMRT.

Another situation in which IMRT may lead to significant dosimetric improvements is that in which the tumor is embedded within or surrounded by a normal tissue exhibiting a dose response with relatively strong volume dependence. An excellent example is lung tumors, the treatment of which is limited primarily by the tolerance of the spinal cord and surrounding normal lung. With conventional multi-field 3DCRT, the beam directions are carefully selected to avoid the spinal cord and to minimize the irradiated volume of normal lung. But beyond beam selection, the user has a limited armamentarium with which to manipulate target coverage and normal tissue dose. Uniform target dose and low normal tissue doses must be achieved using *uniform* or *smoothly varying* intensity patterns from each field (open or wedged fields). In contrast, IMRT combines the *non-uniform* intensity patterns from each field to obtain a *uniform* target dose. This often leads to further decreases in lung dose, particularly at the low or mid dose levels. Figure 6–2 compares 3-D and IMRT dose distributions for a lung tumor. Using identical beam arrangements, similar target coverage is achieved with both plans, but the lung dose is lower with IMRT. As discussed in greater detail in the chapter devoted to the treatment of lung cancer (chapter 12), the improvement in lung dose achieved with IMRT may facilitate dose escalation. In a retrospective review of six patients treated with 3DCRT but re-planned with IMRT by Yorke et al. (Spirou et al. 2001; Yorke 2001), the addition of IMRT would have permitted the prescription

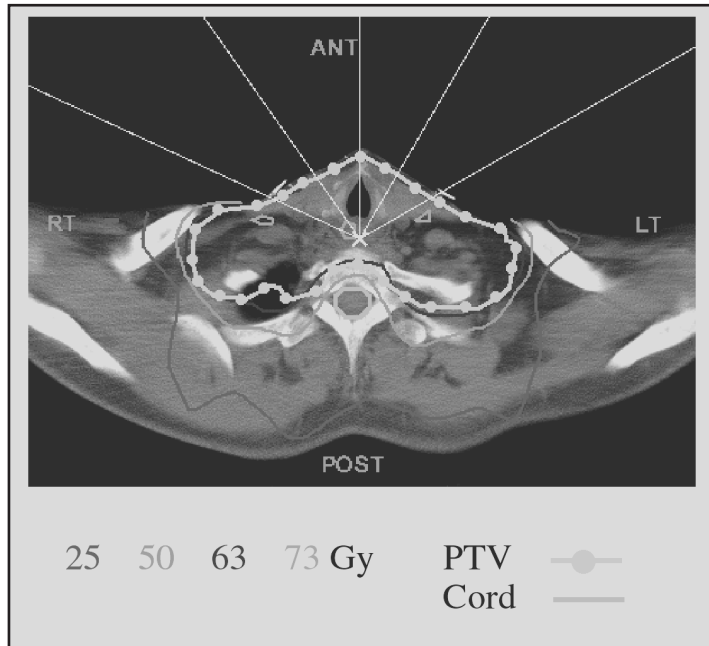


FIGURE 6-1. Five-field IMRT technique for the treatment of thyroid cancer. Note the concave shape of the dose distribution between the target and spinal cord. See COLOR PLATE 10.

dose to be escalated by 13 Gy, on average, for five of six patients. This assumes that the same biological dose limits for the lung would be required for the 3D and IMRT plans.

We have briefly described two clinical scenarios in which IMRT can produce dosimetrically superior distributions. Detailed discussions of these and other IMRT techniques can be found in the site-specific chapters. In some situations, however, the benefits of IMRT may not be as significant

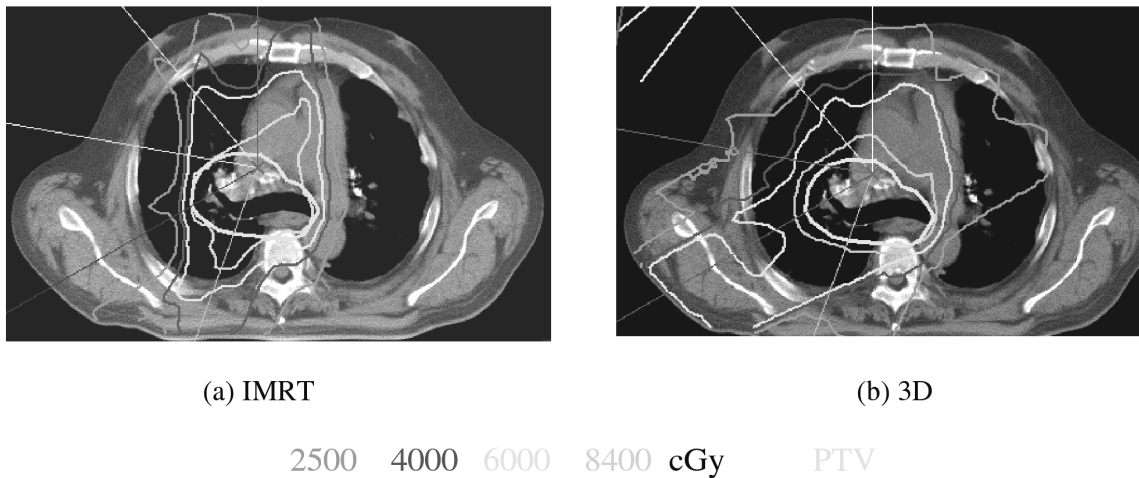


FIGURE 6-2. A comparison of IMRT (a) and 3-D conformal (b) dose distributions for the treatment of a lung tumor. Even though the same beam arrangement was used for both plans, there is significant improvement in the lung dose with IMRT. See COLOR PLATE 11.

and may not warrant the increased cost. Therefore, it is imperative that a critical evaluation of IMRT take place prior to implementation in each clinic. At MSKCC, implementation for a new site is always preceded by a comparison of 3-D and IMRT techniques that, by itself, requires significant physics and physician time. Once the decision to use IMRT is made, a standard beam arrangement and constraint template is defined whenever possible to streamline the routine planning process. We believe that, with IMRT, communication between physicians and planners is crucial. The pre-implementation phase, during which IMRT is compared to other techniques is an ideal time to discuss the goals of treatment and to define, as precisely as possible, the desired target and normal tissues doses.

The MSKCC IMRT Planning Process

Since 1997, IMRT planning at MSKCC has relied on the optimization algorithm developed by Spirou and Chui (1998), which uses conjugate gradient minimization and a least-squares objective function (see also chapter 3). The basic planning steps are described below.

Patient Selection

The vast majority of patients receiving IMRT treatment at MSKCC are treated to sites that have been identified by the department as suitable for this type of treatment. This includes prostate, head and neck, breast, pediatric, para-spinal, and some lung tumors. For these sites, evaluations of the dosimetric benefits of IMRT have been completed and planning procedures have been written that specify the desired target and normal tissue doses and the optimization constraints used to achieve them. Other patients for whom IMRT may be beneficial, by virtue of tumor location, previous radiation treatment, etc., are discussed on a case-by-case basis prior to planning. IMRT treatment to non-routine sites may entail longer planning times (more than one week) since the target and normal tissue constraints must be determined and additional pre-treatment quality assurance (QA) including film dosimetry may be necessary.

Patient Simulation And Structure Localization

Because of the increased conformality of the dose distributions achieved with IMRT, accurate and precise patient treatment is of even more importance than with conventional treatment. All patients undergoing IMRT at MSKCC are immobilized according to tumor location and patient condition. Immobilization methods range from custom foam or thermoplastic molds for prostate, head and neck, and breast patients to stereotactic localization for patients with para-spinal lesions. After immobilization, which takes place either in a conventional simulator or CT simulator room, all patients undergo CT simulation, during which images are acquired throughout the treatment volume and an isocenter is defined. Using the CT (computed tomography) and other appropriate image sets including magnetic resonance or positron emission tomography (MR or PET), the PTV and critical organ contours are defined and transferred along with the images to the planning system.

At the planning system, additional structures used solely to control the dose distribution during optimization are often defined by the planner. Typically, these *optimization only* structures are Boolean combinations of targets and normal tissues. By defining the intersection of targets and normal tissues as separate structures, different prescription doses and constraints can easily be applied to different regions, facilitating the creation of *controlled* dose gradients between normal tissues and targets. Figure 6–3 illustrates the use of Boolean structures in prostate cancer where routinely, the PTV, rectum and PTV-rectal overlap regions are given different constraints during optimization. Special care is taken during this pre-optimization phase to ensure that an adequate number of calculation points are defined within each structure since this influences the optimization results. With the MSKCC algorithm, at least 30 points/cc, distributed quasi-randomly

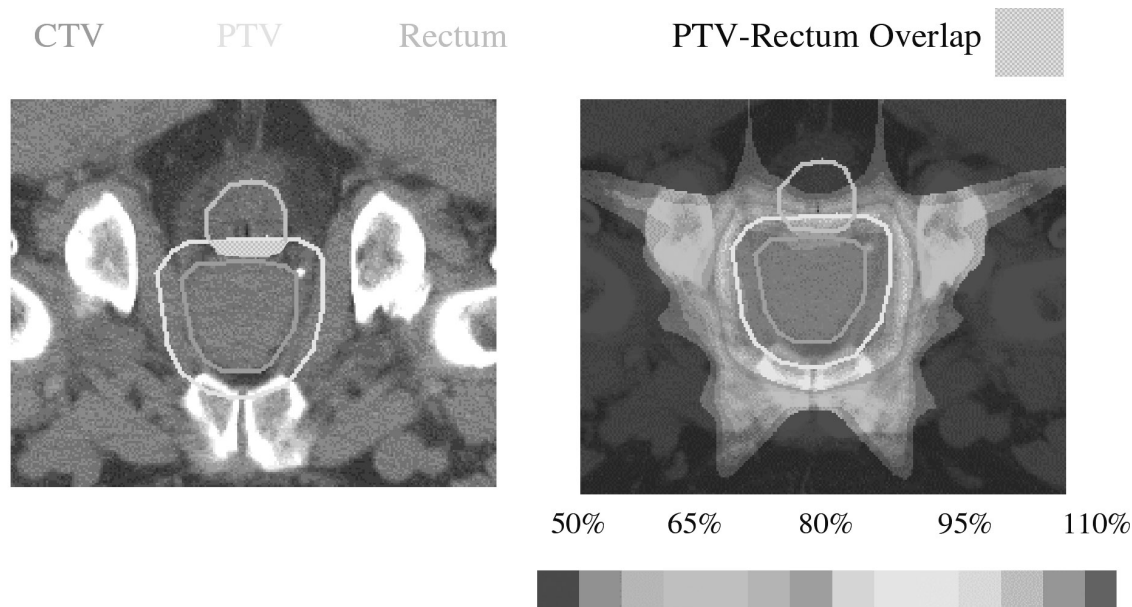


FIGURE 6-3. Use of logical combinations of structures to control optimized dose distributions. See COLOR PLATE 12.

throughout a structure, are needed to ensure results that are independent of point placement. Still, on occasion, portions of a structure, typically narrow outcroppings or thin superior or inferior sections, will be over- or underdosed because of a paucity of calculation points relative to the rest of the structure. Redefining these regions as separate structures for optimization usually eliminates the problem. Further details about the optimization only structures for specific sites are provided in the relevant clinical chapters.

It is important for a clinic implementing a new IMRT program to recognize that the time spent by physicians and planners contouring structures may increase relative to that with 3-D plans. One reason for this is the need to define *optimization only* structures, as discussed above. But additionally, at times, undesirably high doses are delivered to un-contoured normal tissues during optimization. The only way to lower the dose to these tissues is to contour them and to place dose constraints on them during optimization.

Selection Of Beam Energy, Number, And Direction

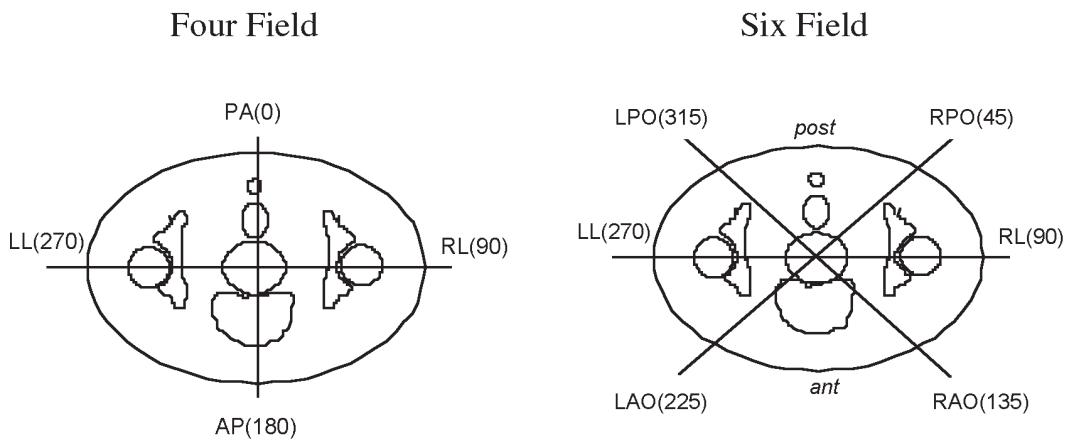
The selection of the optimum number and direction of beams for IMRT may be less critical than for 3DCRT as long as basic concepts are applied. The ability to modulate the beam intensity within a field can partially compensate for a relatively poor choice of beam directions. Since the complexity of treatment often increases as more fields are used, we strive for the best plan with the fewest beams and use the following guidelines:

1. In clinical situations without significant target concavities, a beam arrangement similar to that used for 3DCRT is probably sufficient, and with the addition of IMRT, a superior distribution is often achieved.
2. In the presence of significant target concavities, five to nine uniformly spaced, non-coaxial or, if beneficial, non-coplanar fields, often yield clinically acceptable dose distributions.
3. When selecting IMRT beam directions, attention should be paid to unconstrained normal tissues in the path of the beams. These tissues may receive unacceptably high doses during

optimization that may only be noticed through careful review of dose distributions and dose-volume data.

Some recent discussions have raised the concern that IMRT may increase integral dose due to the increased leakage radiation resulting from longer treatment times and the use of many treatment fields or an arc-type delivery. We would argue that the treatment time for many of the most common IMRT treatments (prostate, for example), is not significantly longer than conventional treatment and that excellent IMRT dose distributions can be achieved without increasing the number of treatment fields. In fact, IMRT, applied to a conventional beam arrangement, may actually decrease integral dose by virtue of its improved conformality. In a recent study of integral dose for prostate patients, Della Bianca evaluated various 3-D and IMRT techniques for 15 prostate patients (Della Bianca, Hunt, and Amols 2002). The integral doses for four (AP, PA, RL, LL) and six-field (RL, LL, RAO, LAO, RPO, LPO) 3-D plans were compared with those for 5, 9, and 13 non-coaxial field IMRT plans (figure 6-4). The five-field IMRT plan yielded the lowest integral dose while a six-field 3-D technique resulted in the highest. Applying intensity modulation to the 3-D four- and six-field beam arrangements decreased the integral dose by as much

3-D Plans:



IMRT Plans:

Number of beams	Gantry Position (degree)
5	0, 75, 135, 225, 285
9	0, 40, 80, 120, 160, 200, 240, 280, 320
13	0, 40, 60, 80, 110, 130, 160, 200, 230, 250, 280, 300, 320
30	Equally distributed every 12 degrees.

FIGURE 6-4. 3-D and IMRT beam arrangements used in the study of integral dose for prostate patients.

as 10%. As a result of the lower path length and improved conformality of the five-field IMRT plan, patients receiving IMRT to 81 Gy would have received approximately the same integral dose as patients treated to 75.6 Gy with a six-field 3DCRT technique.

It has also been suggested that, with IMRT, higher energy x-ray beams (≥ 10 MV) may not be as necessary for deep-seated targets although the recent article by Pirzkall et al. (2002) appears to cast some doubt on this. This study compared IMRT prostate plans for 6, 10, and 18 MV X-rays and found target and rectal doses for 6 MV to be comparable to those obtained with a five-field 18 MV plan, but only if at least nine fields were used. If fewer 6 MV fields were used, the doses to superficial normal tissues were significantly higher than those observed in the higher energy plans.

At MSKCC, no changes in beam energy have been made as IMRT has replaced 3DCRT treatment. Pelvis and abdominal tumors are routinely treated with 15 MV, and lung, breast, head and neck, and pediatric tumors with 6 MV. Breast patients with separations greater than 23 cm are treated using 15 MV X-rays and a beam spoiler or with a mix of 6 and 15 MV beams.

Optimization

A detailed description of the optimization algorithm can be found in chapter 3. Here, a brief description is provided with emphasis on clinical application.

For each treatment field, the collimator is adjusted to enclose the targets with a margin of 1.5 to 2 cm, which prevents the target from lying within the beam penumbra. With the MSKCC algorithm, failure to add this margin may lead to undesirable intensity peaks near the beam edges. An initial dose calculation is performed during which each beam is divided into segments 2 mm wide and 5 mm long and the dose deposition coefficients, a_{ij} representing the dose deposited to i^{th} point in a structure for a unit weight of the j^{th} ray, are calculated. The dose deposition coefficients contain all the information needed by the optimization algorithm to determine the intensity profiles.

The desired dose distribution is described through the optimization parameters (i.e., constraints) for targets and normal tissues. Optimization is achieved by using an iterative process to minimize a quadratic objective function, shown here in a simplified form for a single target:

$$F_{obj} = \frac{1}{N} \left(\sum_j (D_j - C_p)^2 + \sum_k w_k \sum_j \Theta(D_j - C_k) \times (D_j - C_k)^2 \right)$$

where

C_p is the prescription dose for the target.

C_k is the dose of the k^{th} target constraint.

w_k is the user-defined penalty for the k^{th} target constraint.

D_j is the actual dose to the j^{th} point within the target.

N is the number of target points.

$$\Theta(D_j - C_k) = \begin{cases} 1 & \text{if } D_j - C_k < 0 \text{ and } C_k \text{ is a minimum dose constraint} \\ & \text{or } D_j - C_k > 0 \text{ and } C_k \text{ is a maximum dose constraint} \\ 0 & \text{otherwise} \end{cases}$$

For targets, a prescription dose and a *dose window* defining the maximum and minimum dose constraints are allowed. Within this window, a penalty of 1 is applied to deviations from the prescription whereas user-defined penalties are applied outside the window. For critical structures, dose and dose-volume constraints are available. Dose constraints are defined by a maximum dose and penalty while dose-volume constraints are defined by a dose-volume combination and penalty. All MSKCC optimization constraints are so-called *soft* constraints, meaning violation is

possible, but at a *cost* (i.e., penalty). Hard constraints, those that may not be violated under any circumstances, are under development.

At MSKCC, IMRT templates defining the optimization parameters and clinical criteria for all targets and normal tissues are developed for each site prior to large-scale IMRT implementation. These templates are developed primarily through communication between physicians and physicists about the goals and realities of the IMRT treatment and trial-and-error planning on a significant number of test patients. The optimization parameters that define an IMRT template are *average* values, found to yield relatively good dose distributions in a majority of patients. As such, they serve as a starting point for planning individual patients. Invariably, planners must adjust the optimization parameters to *fine tune* the dose distribution for each patient. The templates for the most frequently treated IMRT sites are discussed throughout this book in the site-specific chapters. As an example, the MSKCC 81 Gy prostate template is shown in table 6–1. The optimization parameters are the actual numbers entered into the optimization software while the clinical criteria are used to evaluate the resulting dose distributions and dose-volume histograms (DVHs). It is important to recognize that the selection of optimization parameters is an empirical process and that the MSKCC templates will not necessarily apply to other optimization algorithms.

The importance of devoting significant physician and physicist effort to the development of IMRT templates cannot be stressed enough as their use helps ensure efficient and consistent results for all patients. The response of an optimization algorithm to changes in the optimization parameters is not always intuitive, and even with the use of a template, sub-optimal results can be obtained without the planner realizing it. Optimization algorithm performance studies are one way to get a better understanding of algorithm response and, although time consuming, are highly recommended. A detailed description of the methods and results of one such study that we have recently completed is given later in this chapter in **Controlling Dose Distributions Designed Using Inverse Planning**.

At times, it is useful to modify certain factors affecting the optimization process or the resulting intensity profiles. These include the form of the objective function, the number of iterations performed during optimization, and the profile smoothing method. All these affect the results of optimization and should be investigated as fully as possible prior to clinical implementation. The effect of one of these factors, intensity profile smoothing, is discussed in more detail below.

Intensity profiles may, under certain circumstances, be highly modulated, leading to delivery problems and increased treatment time. They may also deposit unacceptable dose to the critical

Table 6–1. Integral Dose Relative to That for a Five-Field (5F) IMRT Plan, Average Path Length, and Conformity Index for 3-D and IMRT Prostate Treatment Techniques. Data have been averaged over 15 prostate patients

Technique	Gantry Positions (degrees)	Relative Integral Dose (S.D.)	Average Path Length (cm) (S.D.)	Average Conformity Index (S.D.)
4F 3DS	Equally distributed every 90° Start angle = 0° deg.	1.060 (0.05)	15.2 (1.4)	1.48 (0.1)
6F 3D	Equally distributed every 45° Start angle = 45°	1.21 (0.07)	16.3 (1.5) 15.2 (1.4)	1.56 (0.1)
4F IMRT	Same as 4F 3D	0.99 (0.04)	16.3 (1.5)	1.34 (0.09)
6F IMRT	Same as 6F 3D	1.08 (0.04)	15.3 (1.5)	1.36 (0.1)
5F IMRT	0, 75, 135, 225, 285	1	15.0 (1.4)	1.20 (0.06)
9F IMRT	Equally distributed every 40° Start angle = 0°	0.998 (0.01)		1.16 (0.08)
13F IMRT	0, 40, 60, 80, 110, 130, 160, 200, 230, 250, 280, 300, 320	1.04 (0.02)	15.7 (1.4)	1.11 (0.08)
30F IMRT	Equally distributed every 12°	1.03 (0.03)	15.2 (1.3)	1.06 (0.09)

All results indicate average values obtained from 15 patients

¹ Conformity index = $V_{100}(\text{External contour})/V_{100}(\text{PTV})$

organs in the event of setup error or organ motion. Although some modulation is of course necessary, some is a result of numerical artifact, introduced during optimization. To reduce these artifacts, intensity profiles are smoothed, using one of the methods discussed in detail in chapter 3. The default method of smoothing in the MSKCC system (Spirou and Chui 1994) applies a Savitzky-Golay filter (Teukolsky, Vetterling, and Flannery 1992), replacing each ray with a weighted average of itself and its neighbors. This technique significantly reduces the small intensity fluctuations arising from numerical artifact, thereby producing profiles that can be delivered easily in reasonable time. As is the case for all smoothing algorithms however, sharp dose gradients near critical structures are degraded. To minimize this degradation, a second smoothing method (*score smoothing*) was introduced (Spirou et al. 2001) that incorporates a *smoothing* factor in the objective function, thereby smoothing in regions of relatively low dose gradient while preserving the high dose gradient at target-normal tissue interfaces. Dose profiles across a target normal tissue interface for a single field resulting from the Savitzky-Golay and the score smoothing methods are compared in figures 6–5 and 6–6. Both smoothing techniques are used clinically and are chosen based on the following guidelines:

1. When extremely steep dose gradients are not required (e.g., prostate and breast plans), little difference is observed between the Savitzky-Golay and score-smoothing. Therefore, the Savitzky-Golay filter, applied at the end of each iteration, is generally applied since treatment times are minimized.
2. Steep dose gradients, such as those needed in the treatment of recurrent para-spinal or head and neck tumors, may only be achievable with more sophisticated smoothing techniques, i.e., score smoothing. Highly modulated fields delivered dynamically generally require more treatment time and are more prone to beam *hold-offs*. If step-and-shoot delivery is used, a larger number of segments may be necessary.
3. All aspects of treatment, including the effect of treatment uncertainties should be considered before selecting a smoothing technique.

Conversion Of Intensity Profiles To Leaf Motion

IMRT at MSKCC is delivered using dynamic multileaf collimation (DMLC) following the methodology developed by Spirou and Chui (1994), discussed in chapter 3. After optimization, the intensity profiles are converted into 200 segments, requiring that in each segment, at least one leaf move at the maximum allowable speed, thereby minimizing treatment time. Both transmission through the leaves and the effect of the rounded leaf edge of the Varian MLC are considered. Since the original intensity profiles cannot be converted with complete fidelity, the final leaf motion is converted back into a *deliverable* intensity profile for subsequent forward dose calculation and plan evaluation.

Forward Dose Calculation And Plan Evaluation

Once the forward dose calculation is completed using the deliverable profiles, the plan is evaluated using standard methods including planar dose distributions, DVHs, and radiobiological indices such as tumor control probability (TCP) and normal tissue complication probability (NTCP). Additionally, the *DMLC aperture*, an MLC outline defined by the initial and final leaf positions, is created for each field and can be viewed in beam's-eye view with overlaid iso-intensity contours (figure 6–7). If the dose distribution does not meet the clinical goals of treatment, the optimization parameters, optimization only structures, or beams are adjusted and the process is repeated.

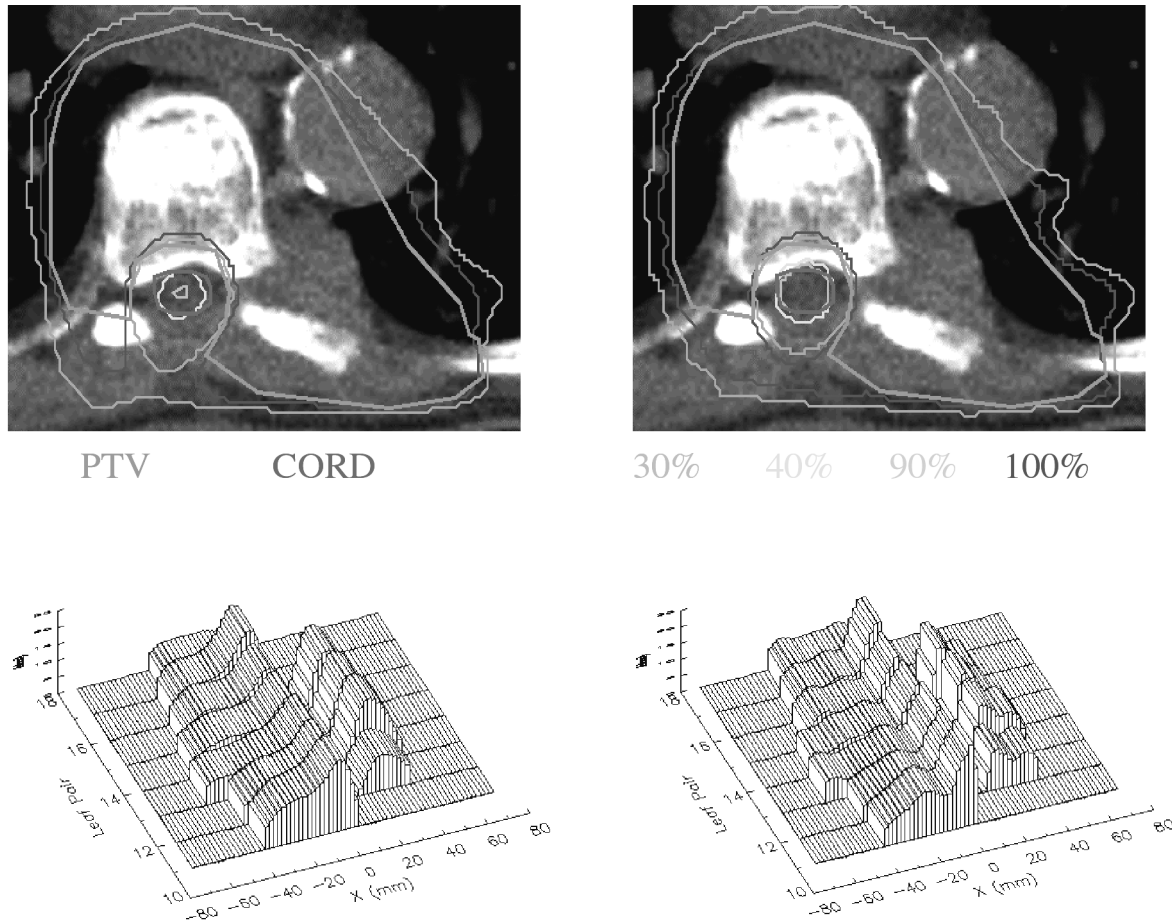
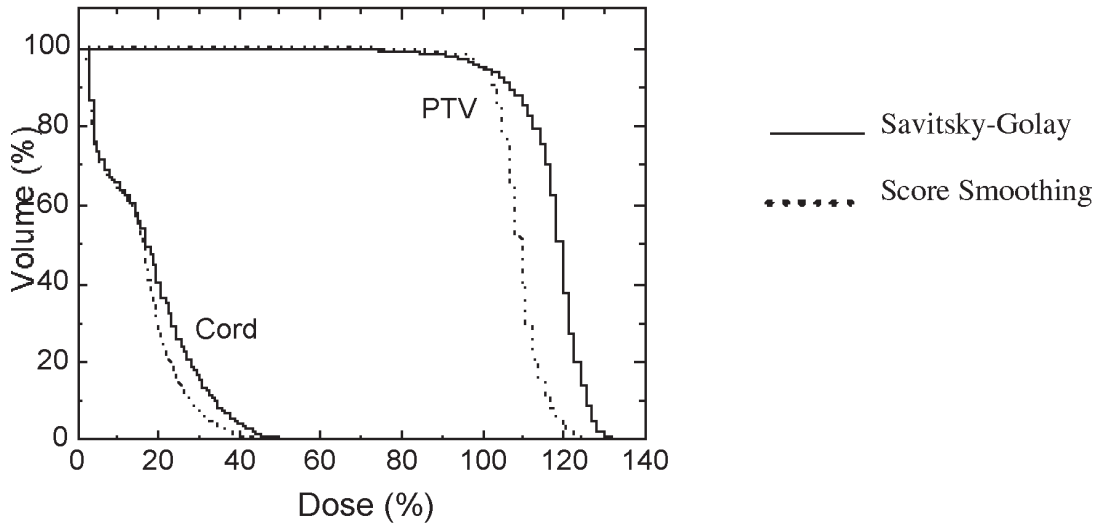


FIGURE 6-5. Effect of two different profile smoothing methods on optimized dose distributions. (a) Profile smoothing performed at end of each iteration (Savitsky-Golay). (b) Profile smoothing performed within the objective function (Score Smoothing). (c) Intensity profiles for posterior beam created by smoothing at the end of each iteration (left) and within the objective function (right). See COLOR PLATE 13.

IMRT Plan Documentation And QA

Upon completion of the plan, monitor unit (MU) settings are calculated and plan documentation is prepared. In addition to the standard documentation, the following is produced for IMRT plans.

1. Digitally reconstructed radiographs (DRRs) of each treatment field overlaid with the DMLC aperture, as described above. These images are compared with portal images, also overlaid with the DMLC aperture, obtained during the patient *setup* prior to the first treatment.
2. Independent verification of the MU setting for each field. As described in chapter 4, a stand-alone software application has been developed for this purpose that accepts, as input, the leaf motion file and MU setting for each field. From the leaf motion file, an intensity profile is generated and the dose to a user-specified point is calculated for comparison with IMRT plan output. Since 1998, this program has provided independent verification of IMRT MU settings and has supplanted the former requirement of film dosimetry for every treatment portal.



Smoothing Method	Total MU (all fields)
After each iteration	891 MU
Within Objective Function	1081 MU

FIGURE 6-6. Dose-volume histograms for the PTV and spinal cord and total MU settings for the Savitsky-Golay and score smoothing techniques for a para-spinal tumor (Figure 6-5).

3. Documentation of the *IMRT plan identification number* embedded in each leaf motion file. This number, which is indexed with each new optimization, is displayed on IMRT plan output including dose distributions and MU calculation sheets.

All IMRT plans are reviewed by a senior physicist prior to the patient’s first treatment. In addition to the standard plan QA, the following is done:

1. Review of the independent MU verification for IMRT fields. Any discrepancy in excess of 2% is initially investigated by calculating doses to additional points with the independent MU software and planning system. Unresolved discrepancies are investigated with film or ion chamber dosimetry.
2. Comparison of the IMRT plan identification number displayed on plan output with that embedded in the leaf motion file for each treatment field. Discrepancies indicate that the leaf motion files do not correspond to those used to create the treatment plan. We believe that a QA check of this type is particularly crucial for institutions (such as MSKCC) using planning systems, electronic charts, and/or record and verify (R&V) systems without integrated databases. On several occasions, we have encountered situations where IMRT plans that were complete and ready for treatment were subsequently modified and planners inadvertently forgot to update the leaf motion files in the electronic chart/R&V system. Fortunately, these

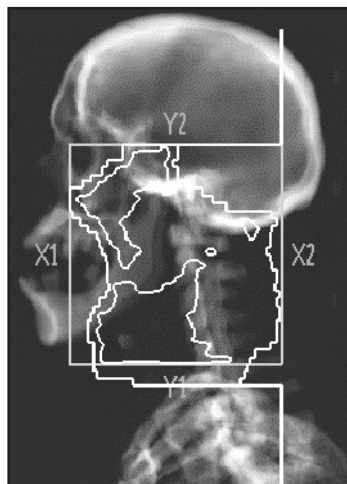


FIGURE 6–7. Digitally reconstructed radiograph demonstrating the DMLC aperture (in white) and iso-intensity line display (in gray).

potentially serious systematic errors were discovered prior to patient filming and treatment through the plan identification number QA procedure.

3. Visual review of color displays of intensity profiles for each treatment field using VARIAN Shaper or VARiS software. Profiles are examined for consistency with expected results and the presence of undesirable intensity peaks.

Controlling Dose Distributions Designed Using Inverse Planning: Optimization Algorithm Performance

Optimized dose distributions are controlled primarily through the beam arrangement, the optimization parameters, and structures. Unfortunately, the response of the optimization algorithm to changes in any of these is not always straightforward or intuitive. Optimization parameters that work well for one patient may produce only mediocre results in another. The modification of a penalty or cost for one structure may affect the dose to another structure not even in the same physical proximity. One thing is for certain: *inverse planning* requires the development of a new set of skills and intuition by the planner. In this section, we will describe some observations and studies that have helped us develop planning skills applicable to the MSKCC optimization algorithm. Although other optimization algorithms may behave quite differently, some of the observations or evaluation methods may be still be applicable.

Optimization Parameters

The goal of the optimization software is to iteratively adjust the beam intensities until the objective function is minimized, and in so doing, satisfy the criteria defined by the optimization parameters. However, often the criteria cannot be satisfied, either because they were physically unrealistic to begin with or because other factors are affecting the relationship between the objective function minimization and the optimization parameters. Our experience has indicated that, in general, optimization parameters must be more stringent than the desired clinical result and that the patient's anatomy, in particular, the proximity of the critical normal tissues to the target, must be considered when setting the optimization parameters.

To improve our understanding of the performance of the optimization software, we have undertaken a pilot study designed to evaluate optimization results for one specific target-normal tissue geometry, that of a concave target surrounding a cylindrical normal tissue (Hunt et al. 2002) (figure 6–8). The variables included the separation between the target and normal tissue and the optimization parameters applied to the normal tissue. The optimized dose distributions were evaluated using the target dose uniformity and maximum normal tissue dose. Figure 6–9 displays the relationship between target and normal tissues doses for target-normal tissue separations of 5 to 13 mm and different optimization parameters. The data points for a particular target-normal tissue separation represent the results obtained with normal tissue dose constraints of 10%, 30%, 50%, and 70% of the prescription. Clearly, the target dose uniformity and normal tissue dose depend strongly on the separation between the two structures, particularly when stringent constraints are placed on the normal tissue dose. If, for example, *acceptable* plans are those in which target dose non-uniformity is no more than 20% and the maximum normal tissue dose is less than 55%, acceptable plans cannot always be achieved. As the separation between the two structures increases, a range of constraints leads to acceptable, but different plans. The determination of the *best* plan still requires a clinical decision based on the balance between target dose uniformity and normal tissue dose.

The effect of varying the penalty placed on the normal tissue rather than the optimization dose is shown in figure 6–10. In general, an increasing penalty was associated with an increase in the PTV uniformity index and little change in the normal tissue dose. A simultaneous lowering of the normal tissue dose and increase in the PTV uniformity index was observed only for

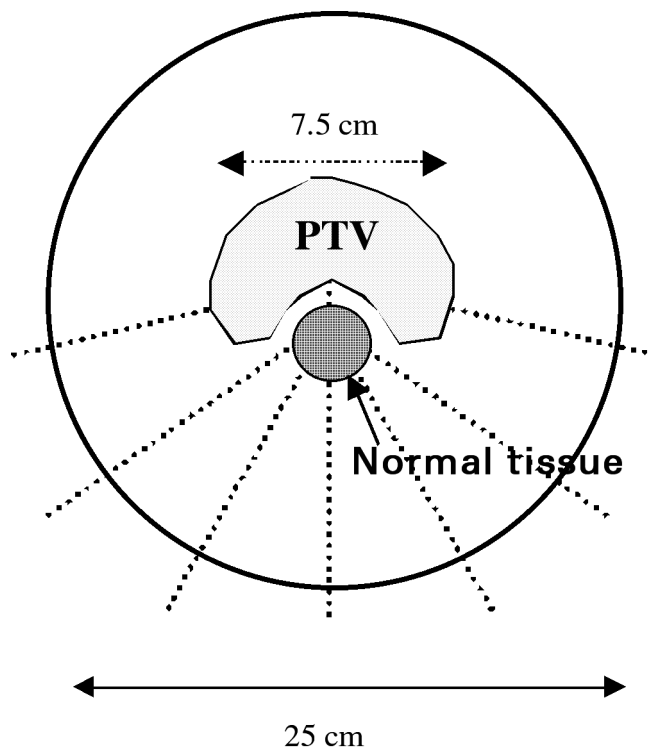


FIGURE 6–8. Phantom, target, and normal tissue geometry used in optimization performance study. A variety of beam arrangements including 5, 7, and 19 equally spaced postero-lateral fields were studied.

small separations and stringent dose limits. Furthermore, optimization results were not as sensitive to changes in the penalty as they were to changes in constraint dose.

Beam Selection

The choice of treatment fields also affects the optimized dose distribution, particularly for concave targets. Increasing the number of fields may lead to an acceptable plan when one is not physically possible with fewer beams. Figure 6–11 shows the effect of increasing the number of postero-lateral fields from 5 to 19 for the concave target-normal tissue geometry shown in figure 6–8. For large target-normal tissue separations and/or relatively large normal tissue doses, increasing the number of fields beyond five has only a minimal effect, consistent with several clinical studies. Nutting et al. (2001) found little change in thyroid distributions when more than five to seven fields were used, although using less than three beams led to a noticeable degradation. Happersett et al. (2000) found five to six fields yielded clinically acceptable target coverage and normal tissue sparing in thyroid IMRT.

If small target-normal tissue separations and steep dose gradients are encountered, however, increasing the number of fields does provide some advantage (figure 6–11). In the treatment of para-spinal tumors, Fournier-Bidoz et al. (2001) found at least nine fields were necessary to achieve very high dose gradients between the target and the spinal cord.

“Optimization Only” Structures

The local distribution of dose, i.e., the location of hot or cold spots or the dose gradient in one specific area, is most easily controlled using artificial structures designed for “optimization only.” For example, we routinely define the intersection of the rectum and the PTV as an

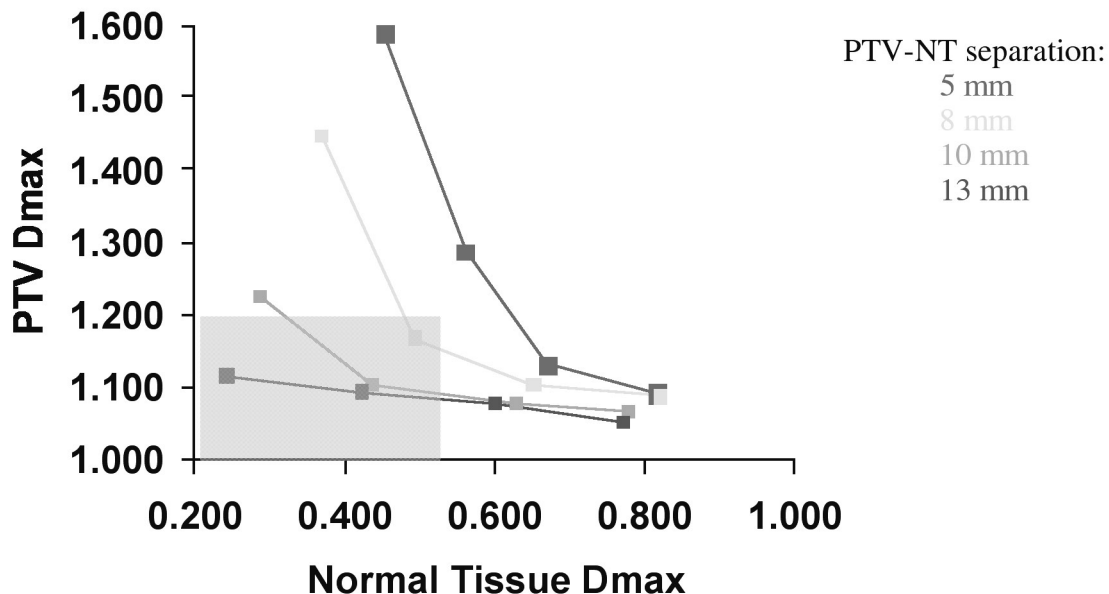


FIGURE 6–9. PTV maximum dose versus maximum normal tissue dose observed with a seven-field beam arrangement and normal tissues positioned 5, 8, 10, and 13 mm from the PTV. Each data point represents the result obtained using a normal tissue dose constraint of 10%, 30%, 50%, or 70% of the prescription and a penalty of 100. PTV constraints remained constant. The shaded region defines “clinically acceptable” plans.

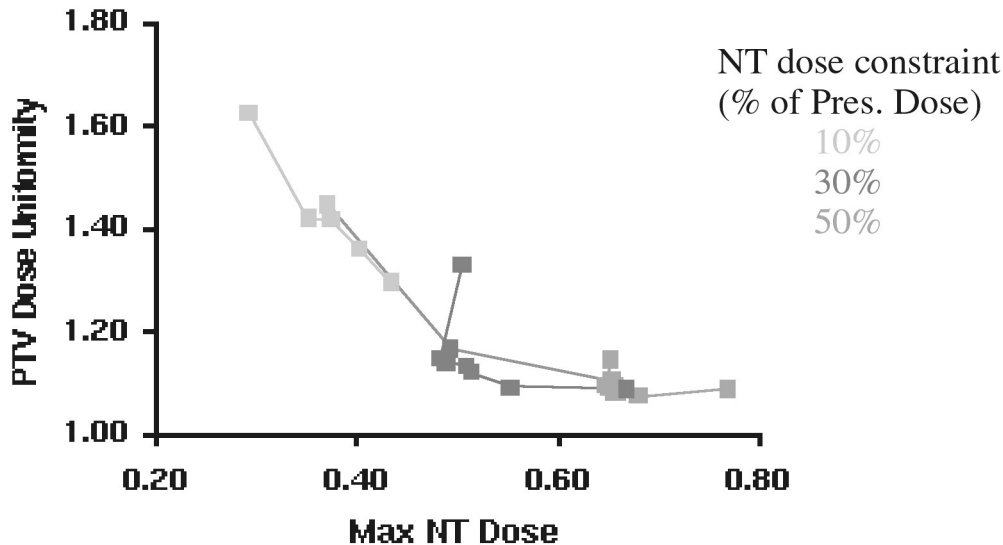


FIGURE 6-10. Effect of modifying the constraint penalty rather than dose for normal tissues positioned 8 mm from the PTV surface. Optimization results obtained with normal tissue dose constraints of 10%, 30%, and 50% of the prescription and a penalty of 100 are joined by the orange solid line. Results for a single dose constraint and penalties varying from 1 to 1000 are indicated by the different color lines.

optimization only structure for prostate patients, as shown in figure 6-3a. Different optimization parameters are prescribed to this region of the PTV (table 6-2) in order to create a well-defined dose gradient between the posterior aspect of the prostate and the anterior rectal wall (figure 6-3b).

Optimization only structures may also be useful in achieving the steepest dose gradient between two structures. In an evaluation of IMRT for para-spinal tumors, Fournier-Bidoz et al. (2001) found that optimizations using *rinds* of the PTV and adjacent spinal cord led to steeper dose gradients between the two structures than optimizations using the whole structures. For a single field, the dose gradient between the target and critical structure was improved by approximately 1.5%/mm when rinds were used.

Summary

Although many steps in the planning process for IMRT treatments are similar to those for 3-D conformal treatments, the creation of the actual treatment plan, (i.e., the optimization or inverse planning process) differs significantly and requires planners and physicians to develop new technical skills and ways of thinking about treatment planning. Initially, this method of planning may not be intuitive and, therefore, may take substantially longer than conventional 3-D planning. Eventually, though, if the planners and physicians work together to develop constraint templates and class solutions for situations where they are feasible, IMRT planning will become more “routine” and can normally be completed in approximately the same time as 3-D plans.

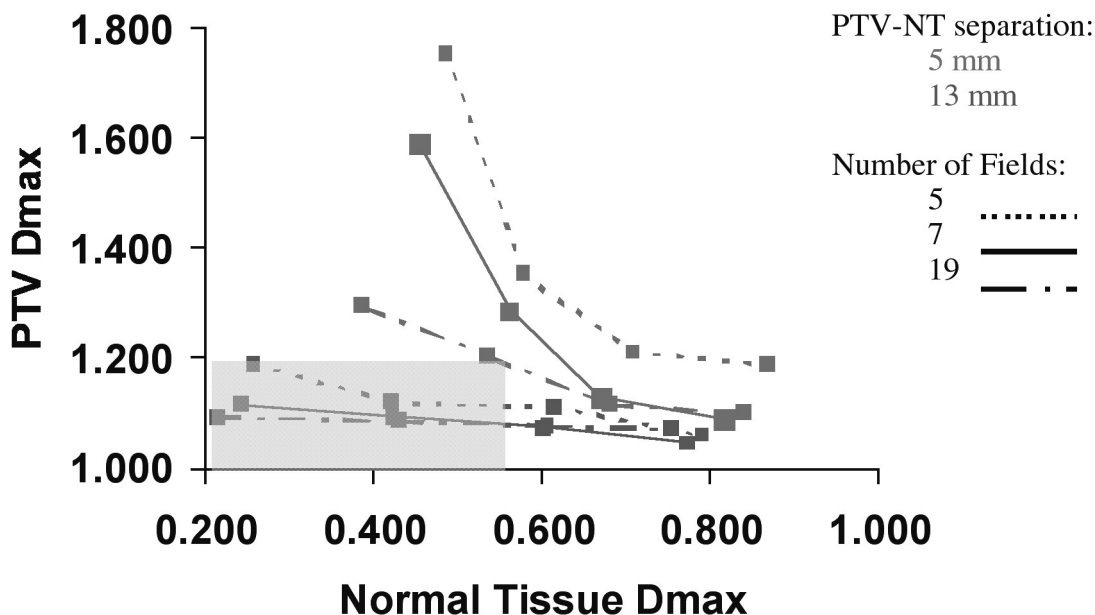


FIGURE 6–11. Effect of the number of treatment fields on optimization results for normal tissues positioned 5 and 13 mm from the PTV. Results for 5, 7, and 19 equally spaced beam arrangements directed from the posterior and postero-lateral directions are shown. The shaded area represents “clinically acceptable” plans.

Table 6–2. MSKCC IMRT Template for 81 Gy Prostate Patients: The IMRT Template Defines the Parameters That Are Used as a Starting Point for Optimization and the Criteria Used to Evaluate the Plan

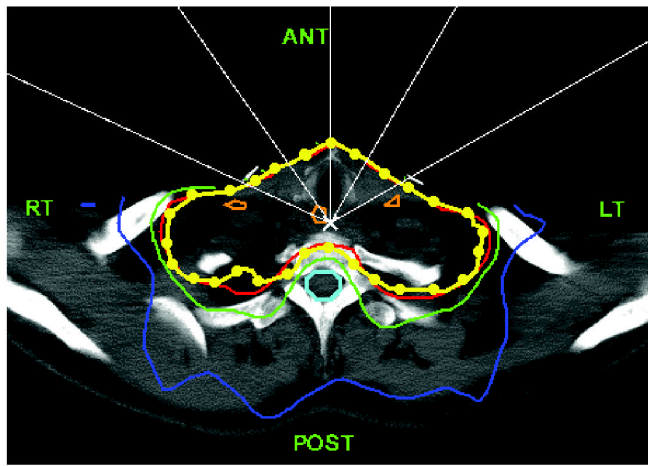
Structure	Optimization Parameters			Treatment Plan Criteria	
	Max. Dose/Penalty	Min Dose/Penalty	Volume (%)	Dose	Volume (%)
PTV (excluding Rectal Overlap)	82.6 Gy/50	79.4 Gy/50	—	90 Gy Max.	V95>90
PTV-Rectum Overlap Region	77.8 Gy/20	75.3 Gy/10	—	—	—
Rectal Wall	77 Gy/20	—	—	75.6 Gy	30
Rectal Wall	32.4 Gy/20	—	30	47 Gy	53
Bladder Wall	79.4 Gy/35	—	—	—	—
Bladder Wall	32.4 Gy/20	—	30	40 Gy	60

References

- Armstrong, J. G., C. Burman, S. Leibel, D. Fontenla, G. Kutcher, M. Zelefsky, and Z. Fuks. (1993). “Three-dimensional conformal radiation therapy may improve the therapeutic ratio of high dose radiation therapy for lung cancer.” *Int. J. Radiat. Oncol. Biol. Phys.* 26:685–689.
- Bortfeld, T., J. Burkelbach, R. Boesecke, and W. Schlegel. (1990). “Methods of image reconstruction from projections applied to conformation radiotherapy.” *Phys. Med. Biol.* 35: 1423–1434.

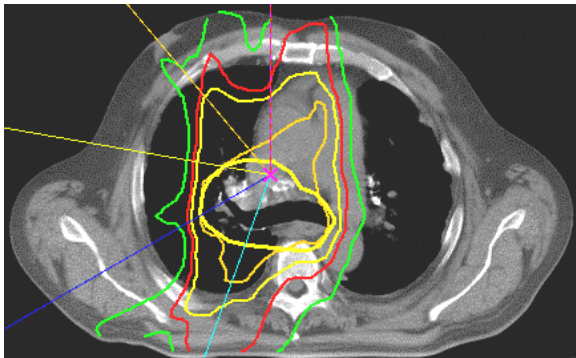
- Boyer, A. L., T. Bortfeld, D. L. Kahler, and T. J. Waldron. "MLC Modulation of X-ray Beams in Discrete Steps" in *XIth International Conference on the Use of Computers in Radiation Therapy*. A. R. Hounsell, J. M. Wilkinson, and P. C. Williams (eds.). March 20–24, 1994. Manchester, UK. Manchester, UK: Christie Hospital NHS Trust. Madison, WI: Medical Physics Publishing, pp. 180–181, 1994.
- Brahme, A. (1988). "Optimization of stationary and moving beam radiation therapy techniques." *Radiother. Oncol.* 12(2):129–140.
- Burman, C., C. S. Chui, G. Kutcher, S. Leibel, M. Zelefsky, T. LoSasso, S. Spirou, Q. Wu, J. Yang, J. Stein, R. Mohan, Z. Fuks, and C. C. Ling. (1997). "Planning, delivery, and quality assurance of intensity-modulated radiotherapy using dynamic multileaf collimator: A strategy for large-scale implementation for the treatment of carcinoma of the prostate." *Int. J. Radiat. Oncol. Biol. Phys.* 39(4):863–873.
- Carol, M. "Integrated 3-D Conformal Multivane Intensity Modulation Delivery System for Radiotherapy" in *XIth International Conference on the Use of Computers in Radiation Therapy*. A. R. Hounsell, J. M. Wilkinson, and P. C. Williams (eds.). March 20–24, 1994. Manchester, UK. Manchester, UK: Christie Hospital NHS Trust. Madison, WI: Medical Physics Publishing, pp. 172–173, 1994.
- Carol, M. P., R. V. Nash, R. C. Campbell, R. Huber, and E. Sternick "The Development of a Clinically Intuitive Approach to Inverse Treatment Planning: Partial Volume Prescription and Area Cost Function" in *XII ICCR: XII International Conference on the Use of Computers in Radiation Therapy*. D.D. Leavitt and G. Starkschall (eds). Salt Lake City, Utah, May 27–30, 1997. Madison, WI: Medical Physics Publishing, pp. 317–319, 1997.
- Chao, K. S., D. A. Low, C. A. Perez, and J. A. Purdy. (2000). "Intensity-modulated radiation therapy in head and neck cancers: The Mallinckrodt experience." *Int. J. Cancer* 90(2):92–103.
- Chui, C. S., M. F. Chan, E. Yorke, S. Spirou, and C. C. Ling. (2001). "Delivery of intensity-modulated radiation therapy with a conventional multileaf collimator: Comparison of dynamic and segmental methods." *Med. Phys.* 28(12): 2441–2449.
- Della Bianca, C., M. Hunt, and H. Amols. (2002). "A comparison of the integral dose from 3D conformal and IMRT techniques in the treatment of prostate cancer." (Abstract). *Med. Phys.* 29(6):1216.
- De Neve, W., W. De Gersem, S. Derycke, C. De Meerleer, M. Moerman, M. T. Bate, B. Van Duyse, L. Vakaet, Y. De Deene, B. Mersseman, C. De Wagter, and C. De Waeter. (1999). "Clinical delivery of intensity modulated conformal radiotherapy for relapsed or second-primary head and neck cancer using a multileaf collimator with dynamic control." *Radiother. Oncol.* 50(3):301–314.
- Ezzell, G. A. (1996). "Genetic and geometric optimization of three-dimensional radiation therapy treatment planning." *Med. Phys.* 23(3): 293–305.
- Fournier-Bidoz, N., P. Giraud, S. Spirou, C. Chui, M. Lovelock, K. Yenice, and M. Hunt. (2001). "Penumbra sharpening with IMRT in Paraspinal Treatments." (Abstract). *Med. Phys.* 28(6):1260.
- Galvin, J. M., X. G. Chen, and R. M. Smith. (1993). "Combining multileaf fields to modulate fluence distributions." *Int. J. Radiat. Oncol. Biol. Phys.* 27(3): 697–705.
- Happersett, L., M. Hunt, C. Chui, C. Burman, C. Ling, M. Zelefsky, S. Leibel, and H. Amols. (1999). "Dose painting for prostate cancer using IMRT techniques." American Association of Physicists in Medicine (AAPM) Annual Meeting, Nashville, TN, June 1999. *Med. Phys.* 26(6): No page number.
- Happersett, L., M. Hunt, L. Chong, et al. (2000). "Intensity Modulated radiation therapy for the treatment of thyroid cancer." *Int. J. Radiat. Oncol. Biol. Phys.* 48(3S):351.
- Hsiung, C. Y., E. D. Yorke, C. S. Chui, M. A. Hunt, C. C. Ling, E. Y. Huang, C. J. Wang, H. C. Chan, S. A. Yeh, H. C. Hsu, and H. I. Amols. (2002). "Intensity-modulated radiotherapy versus conventional three-dimensional conformal radiotherapy for boost or salvage treatment of nasopharyngeal carcinoma." *Int. J. Radiat. Oncol. Biol. Phys.* 53(3):638–647.
- Hunt, M. A., M. J. Zelefsky, S. Wolden, C. S. Chui, T. LoSasso, K. Rosenzweig, L. Chong, S. V. Spirou, L. Fromme, M. Lumley, H. Amols, C. C. Ling, and S. A. Leibel. (2001). "Treatment planning and delivery of intensity-modulated radiation therapy for primary nasopharynx cancer." *Int. J. Radiat. Oncol. Biol. Phys.* 49(3):623–632.
- Hunt, M., C. Y. Hsiung, S. V. Spirou, C. S. Chui, and C. C. Ling. (2002). "Evaluation of concave dose distributions created using an inverse planning system." *Int. J. Radiat. Oncol. Biol. Phys.* 54(3):953.
- Langer, M., and J. Leong. (1987). "Optimization of beam weights under dose-volume restrictions." *Int. J. Radiat. Oncol. Biol. Phys.* 13(8): 1255–1260.

- Llacer, J. (1997). "Inverse radiation treatment planning using the dynamically penalized likelihood method." *Med. Phys.* 24(11):1751–1764.
- Mageras, G. S., and R. Mohan. (1993). "Application of fast simulated annealing to optimization of conformal radiation treatments." *Med. Phys.* 20(3): 639–647.
- Nutting, C. M., D. J. Convery, V. P. Cosgrove, C. Rowbottom, L. Vini, C. Harmer, D. P. Dearnaley, and S. Webb. (2001). "Improvements in target coverage and reduced spinal cord irradiation using intensity-modulated radiotherapy (IMRT) in patients with carcinoma of the thyroid gland." *Radiother. Oncol.* 60(2):173–180.
- Pirzkall, A., M. P. Carol, B. Pickett, P. Xia, M. Roach 3rd, L. J. Verhey. (2002). "The effect of beam energy and number of fields on photon-based IMRT for deep-seated targets." *Int. J. Radiat. Oncol. Biol. Phys.* 53(2):434–442.
- Purdy, J. A. "The Development of Intensity Modulated Radiation Therapy" in *1st NOMOS IMRT Workshop*. Durango, Colorado. Madison, WI: Advanced Medical Publishing, 1997.
- Rosen, I. I., K. S. Lam, R. G. Lane, M. Langer, and S. M. Morrill. (1995). "Comparison of simulated annealing algorithms for conformal therapy treatment planning." *Int. J. Radiat. Oncol. Biol. Phys.* 33(5):1091–1099.
- Soderstrom, S., and A. Brahme. (1992). "Selection of suitable beam orientations in radiation therapy using entropy and Fourier transform measures." *Phys. Med. Biol.* 37(4): 911–924.
- Spirou, S. V., and C. S. Chui. (1994). "Generation of arbitrary intensity profiles by dynamic jaws or multi-leaf collimators." *Med. Phys.* 21(7): 1031–1041.
- Spirou, S. V., and C. S. Chui. (1998). "A gradient inverse planning algorithm with dose-volume constraints." *Med. Phys.* 25(3):321–333.
- Spirou, S., E. Yorke, A. Jackson, and C. Chui. (2001). "Optimization with both dose-volume and biological constraints for lung IMRT." 43rd Annual AAPM Meeting, Salt Lake City, UT, July 22–26, 2001. *Med. Phys.* 28(6):1261.
- Spirou, S. V., N. Fournier-Bidoz, J. Yang, C. S. Chui, and C. C. Ling. (2001). "Smoothing intensity-modulated beam profiles to improve the efficiency of delivery." *Med. Phys.* 28(10):2105–2112.
- Teukolsky, S., W. Vetterling, and B. Flannery. *Savitzky-Golay Smoothing Filters, in Numerical Recipes in C*. New York: W.H. Press, pp. 650–655, 1992.
- Verhey, L. J. (1999). "Comparison of three-dimensional conformal radiation therapy and intensity-modulated radiation therapy systems." *Semin. Radiat. Oncol.* 9(1):78–98.
- Vijayakumar, S., L. C. Myriantopoulos, I. Rosenberg, H. J. Halpern, N. Low, and G. T. Chen. (1991). "Optimization of radical radiotherapy with beam's eye view techniques for non-small cell lung cancer." *Int. J. Radiat. Oncol. Biol. Phys.* 21(3):779–788.
- Wu, Q., M. Manning, R. Schmidt-Ullrich, and R. Mohan. (2000). "The potential for sparing of parotids and escalation of biologically effective dose with intensity-modulated radiation treatments of head and neck cancers: A treatment design study." *Int. J. Radiat. Oncol. Biol. Phys.* 46(1):195–205.
- Yorke, E. (2001). "Advantages of IMRT for dose escalation in radiation therapy of lung cancer." 43rd Annual AAPM Meeting, Salt Lake City, UT, July 22–26, 2001. *Med. Phys.* 28(6):1291–1292.
- Zelevsky, M. J., Z. Fuks, L. Happersett, H. J. Lee, C. C. Ling, C. M. Burman, M. Hunt, T. Wolfe, E. S. Venktraman, A. Jackson, M. Skwarchuk, and S. A. Leibel. (2000). "Clinical experience with intensity modulated radiation therapy (IMRT) in prostate cancer." *Radiother. Oncol.* 55(3):241–249.

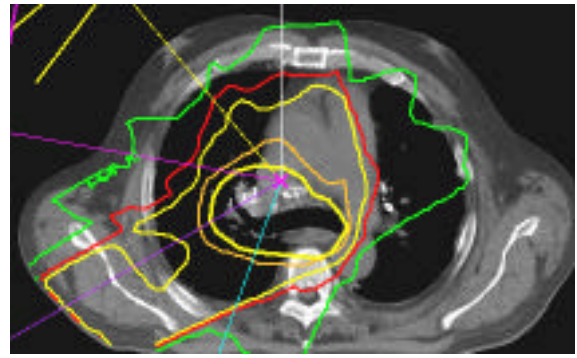


25 50 63 73 Gy PTV Cord

COLOR PLATE 1. Figure 6-1. Five-field IMRT technique for the treatment of thyroid cancer. Note the concave shape of the dose distribution between the target and spinal cord.



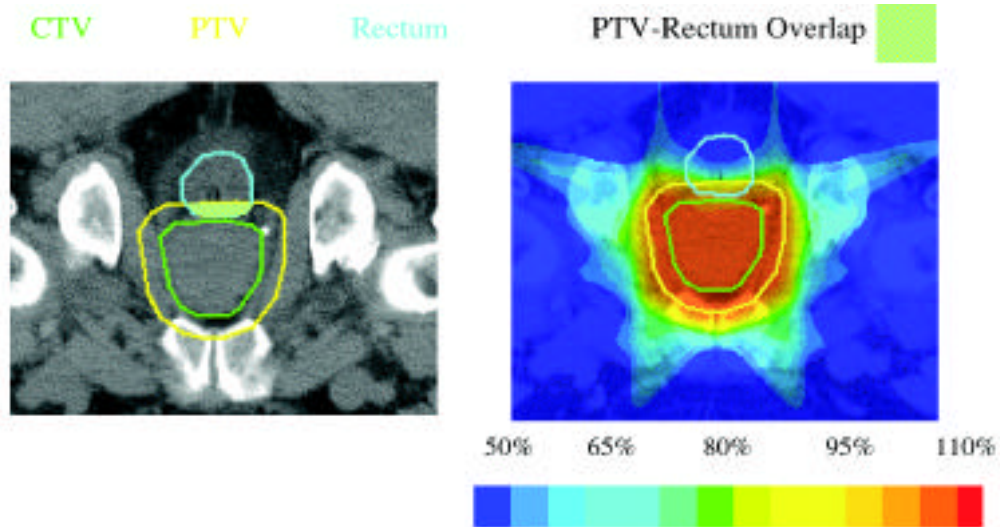
(a) IMRT



(b) 3D

2500 4000 6000 8400 cGy PTV

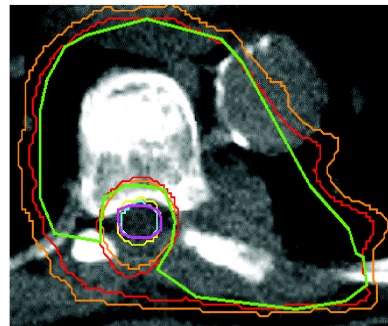
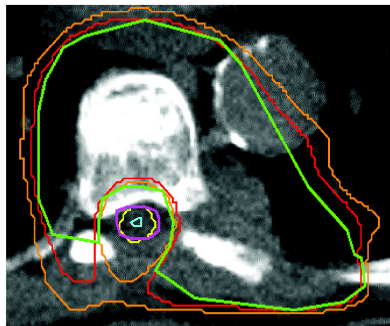
COLOR PLATE 2. Figure 6-2. A comparison of IMRT (a) and 3-D conformal (b) dose distributions for the treatment of a lung tumor. Even though the same beam arrangement was used for both plans, there is significant improvement in the lung dose with IMRT.



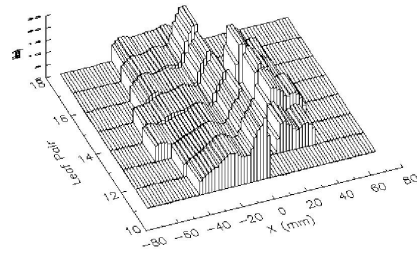
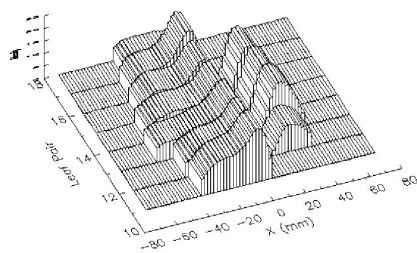
COLOR PLATE 3. Figure 6-3. Use of logical combinations of structures to control optimized dose distributions.

(a). Profile smoothing performed at end of each iteration (Savitsky-Golay)

(b). Profile smoothing performed within the objective function (Score smoothing)



PTV CORD — 100 — 90 — 40 — 30



(c). Intensity profiles for posterior beam created by smoothing at the end of each iteration (left) and within the objective function (right).

COLOR PLATE 4. Figure 6-5. Effect of two different profile smoothing methods on optimized dose distributions. (a) Profile smoothing performed at end of each iteration (Savitsky-Golay). (b) Profile smoothing performed within the objective function (Score Smoothing). (c) Intensity profiles for posterior beam created by smoothing at the end of each iteration (left) and within the objective function (right).